FULL PAPER

Dalton
www.rsc.org/dalton

The structural mobility of zinc complexes with tetradentate tripodal ligands derived from the amino acids glycine and phenylalanine †

Nicole Niklas, Achim Zahl and Ralf Alsfasser *
Institute of Inorganic Chemistry, University of Erlangen-Nürnberg, Egerlandstr. 1, D-91058 Erlangen, Germany. E-mail: alsfasser@chemie.uni-erlangen.de; Fax: 49-9131-8527387

Received 5th December 2002, Accepted 21st January 2003
First published as an Advance Article on the web 6th February 2003

Crystallographic studies indicate that aromatic interactions favor the formation of trigonal-bipyramidal zinc(II) complexes with the tetradentate tripodal ligand bpaAc–Phe–OMe (*N*,*N*-bis(2-picolyl)aminoacyl-(*S*)-phenylalanine-methylester). The benzyl side chain in $[(bpaAc–Phe–OMe)Zn(OTf)]^+$ (**1b**, OTf = triflate), $[(bpaAc–Phe–OMe)Zn(H_2O)]^{2+}$ (**2b**) and $[(bpaAc–Phe–OMe)Zn(pz)]^{2+}$ (**3b^t**, pz = pyrazole; t = trigonal-bipyramidal) is oriented towards the axial active coordination site with the phenyl ring *ca.* 4.5 Å away from the metal center. Here we show that this conformation is retained in solutions of **1b**, **2b** and $[(bpaAc–Phe–OMe)Zn(Cl)]^+$ (**8b**). Temperature-dependent ^{1}H NMR spectra reveal that the phenylalanine side chain is locked in its position as long as the coordination sphere stays trigonal-bipyramidal. Based on our crystallographic results we expected the pyrazole and *N*-methylimidazole complexes **3b^t** and $[(bpaAc–Phe–OMe)Zn(N\text{-}Meim)]^{2+}$ (**4b^t**, *N*-Meim = *N*-methylimidazole) to be labile with respect to addition of a sixth ligand such as triflate, water, pyrazole or *N*-methylimidazole. ^{1}H NMR studies confirm that the six-coordinate species **3b^o** and **4b^o** (o: octahedral) are formed in solution. This is presumably due to solvation effects and mobilizes the benzyl side chain which is flexible in octahedral complexes.

Introduction

It is still one of the most challenging goals of synthetic coordination chemistry to achieve control over the stereochemistry of metal complexes. Much can be learned from biological systems which feature numerous weak non-covalent interactions for the structural stabilization of bioinorganic assemblies.[1] Among those, aromatic π–π stacking and cation–π interactions are of particular importance. Common knowledge is the base stacked structure of the DNA double helix.[2] Similarly important is the ubiquitous structural role of aromatic interactions in proteins and biological receptors.[3] Recent results show that aromatic interactions also occur between coordinated ligands and aromatic amino acids in metalloproteins.[4] The results from biochemical research have stimulated numerous studies on synthetic systems which range from the structure of benzene[5] to host–guest chemistry.[6] Accounts on π–π stacking[7] and CH–π interactions[8] in the second coordination sphere of metal complexes have recently been published. Several reports exist on bioinorganic model compounds with a particular focus on copper complexes with aromatic amino acids.[9] The potential of aromatic interactions to fine tune the chemical and physical properties of metal complexes is evident from the stabilization of ternary metal complexes,[10] stereoselective complex formation reactions,[11] and the mediation of magnetic interactions in the solid state.[12]

In our work on amino acid derived tripodal ligands[13] we started to exploit the remarkable features of aromatic interactions by using phenylalanine as a building block in metal complexes. In a recent paper we have presented a series of crystal structures which indicate that the ligand (bispicolyl)-aminoacyl phenylalanine methylester (bpaAc–Phe–OMe) exhibits a remarkable preference for trigonal-bipyramidal geometries in its zinc complexes.[14] A representative structure is shown in Fig. 1.

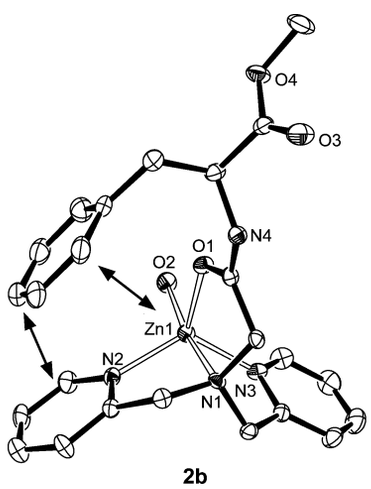

2b

Fig. 1 Structure of $[(bpaAc–Phe–OMe)Zn(OH_2)]^{2+}$; π–π and π–cation interactions are indicated as arrows.

The benzyl side chain is always located 4.5 Å away from the metal center and above one of the pyridine rings. This orientation suggests that cation–π and π–π interactions involving the metal center and one of the pyridine rings are relevant. A crucial test for this hypothesis is the maintenance of the solid state structures in solution. Temperature-dependent ^{1}H NMR studies on zinc complexes with the ligands bpaAc–Phe–OMe and bpaAc–Gly–OEt have therefore been performed. The results are presented in the following report.

Results and discussion

Complexes

Starting points for our investigations were the published compounds shown in Scheme 1.[13,14] It is important for the following to recall some of our earlier results.[14] We have studied the substitution of a triflato ligand ($SO_3CF_3^-$) in trigonal-bipyramidal complexes of the type $[(bpaAc–AA–OR)Zn(SO_3CF_3)]^+$ (**1a**:

† Electronic supplementary information (ESI) available: Fig. S1: ^{1}H NMR spectra ($CDCl_3$ solutions) of the bpaAc–Phe–OMe complexes **1b/2b**, **3b^o**, **5b** and **8b** at room temperature. See http://www.rsc.org/suppdata/dt/b2/b212049f/

DOI: 10.1039/b212049f

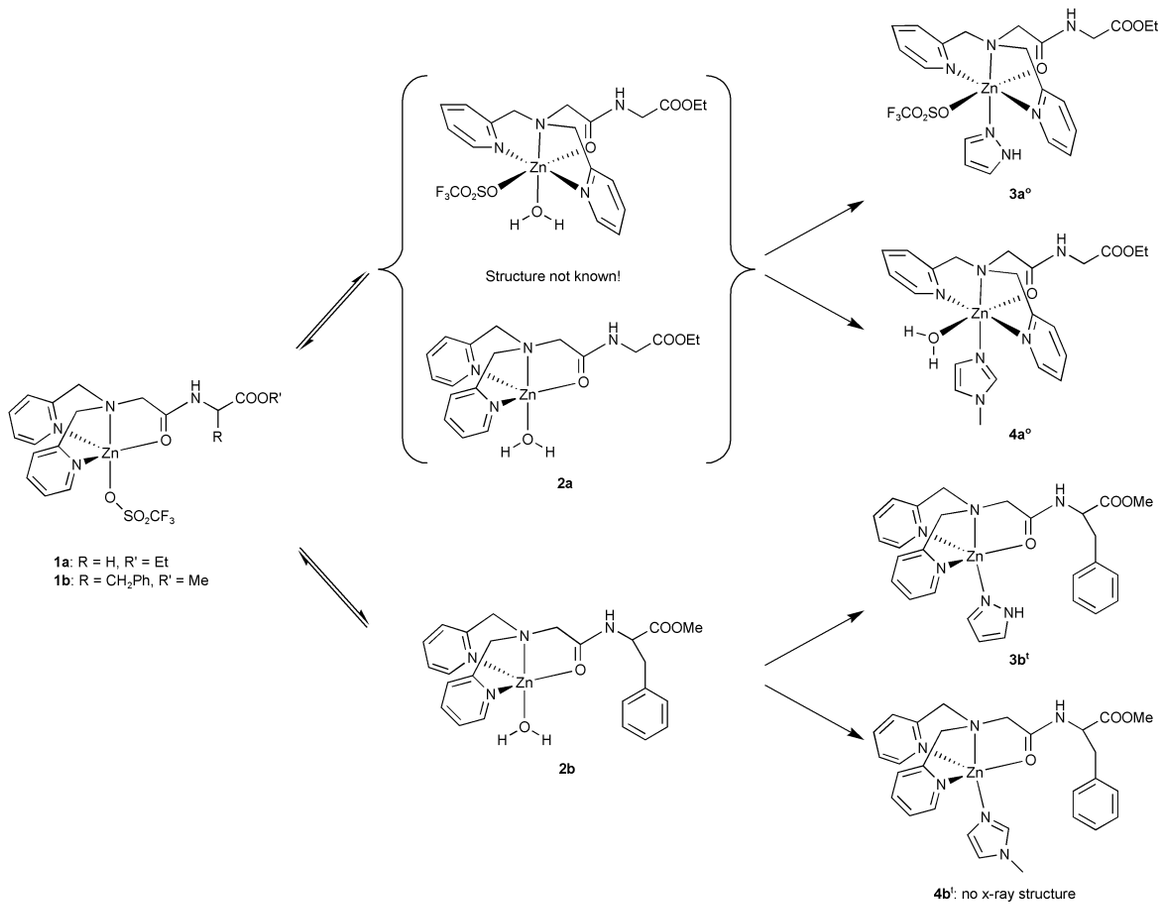

Scheme 1 Zinc complexes of the ligands bpaAc–Gly–OEt (**1a**–**4a**) and bpaAc–Phe–OMe (**1b**–**4b**).

AA–OR=Gly–OEt; **1b**: AA–OR=Phe–OMe). X-Ray structures were obtained for all complexes except **2a** and **4b**. If moisture is not rigorously excluded the triflato complexes **1a** and **1b** rapidly equilibrate with their aqua derivatives **2a** and **2b**, respectively. Since the presence of water was generally beneficial we did not take precautions and will later write **1a/2a** (**1b/2b**) to indicate that the two species coexist in solution. X-ray crystallography showed that the aqua complex $[(bpaAc–Phe–OMe)Zn(H_2O)]^{2+}$ (**2b**) remains trigonal-bipyramidal but exhibits a significantly bent *trans*-N–Zn–OH_2-axis (170°) compared with analogous triflato and chloro complexes (177°). Despite considerable efforts we were not able to crystallize the corresponding glycine derivative **2a**. This is particularly unfortunate since interesting differences are observed between the glycine and the phenylalanine ligand in pyrazole (**3a°**, **b'**; o: octahedral, t: trigonal-bipyramidal) and imidazole (**4a°**, **4b'**) complexes. Whereas octahedral complexes are formed with bpaAc–Gly–OEt, the ligand bpaAc–Phe–OMe stabilizes a distorted trigonal-bipyramidal coordination sphere, presumably by aromatic π–cation and π–π-interactions.[3d,e] The structure of **3b** is characterized by an even more pronounced bending of the *trans*-N–Zn–L-axis (165°) compared with **2b**. A comparison of the different structures has led us to propose a well defined reaction trajectory for the conversion of trigonal-bipyramidal to octahedral species in our series.[14] Fig. 2 shows how the *trans*-N–Zn–L-axis bends

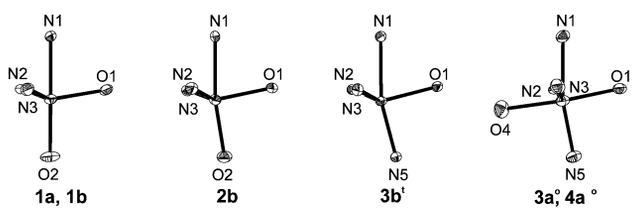

Fig. 2 Conversion of trigonal-bipyramidal to octahedral zinc complexes.

(**1a**,**b**: 177°; **2b**: 170°; **3b'**: 165°; **3a°**,**4a°**: 167°) before a small opening of the pyridine ligands accommodates the incoming sixth ligand. The compound **3b'** is well pre-organized to bind an additional ligand. We have therefore interpreted its structure as a transition state analogue which is stabilized by non-covalent aromatic interactions.

The results summarized above pose two questions. First, it is important to know whether the proposed aromatic interactions are strong enough to be relevant in solution. If so, a locked conformation of the benzyl side chain in trigonal-bipyramidal structures would be expected. Secondly, particularly interesting cases are the "transition state" structures **3b'** and **4b'**. One would expect that these compounds are easily converted to octahedral species at room temperature in solution if the proposed reaction trajectory is valid.

In order to evaluate these questions we have performed a number of synthetic and mechanistic studies. We will summarize the preparative and structural results first in order to facilitate the discussion of the NMR studies in section below. Our first goal was the preparation of definitive octahedral complexes with the ligand bpaAc–Phe–OMe. We have therefore set out to study compounds containing two aromatic heterocyclic coligands. The results are shown in Scheme 2.

In solution, the amine complexes **3a°**,**b'** and **4a°**,**b'** react with a second equivalent of pyrazole or *N*-methylimidazole to form octahedral complexes of the general formula $[(bpaAc–AA–OR)Zn(L')(L'')]^{2+}$ (**5**: L′ = L″ = pz; **6**: L′ = L″ = *N*-Meim; **7**: L′ = pz, L″ = *N*-Meim; **a:** bpaAc–Gly–OEt; **b**: bpaAc–Phe–OMe). This is evident from the ^{1}H NMR spectra which always show the presence of two undistinguishable aromatic amine ligands. The complexes **5a/b** and **6a/b** are also formed from **1a/2a** and **1b/2b** by addition of the appropriate stoichiometric amounts of pyrazole and *N*-methylimidazole, respectively. However, attempts to isolate and purify the products have only been successful in the case of $[(bpaAc–Gly–OEt)Zn(im)_2]^{2+}$ (**6a**).

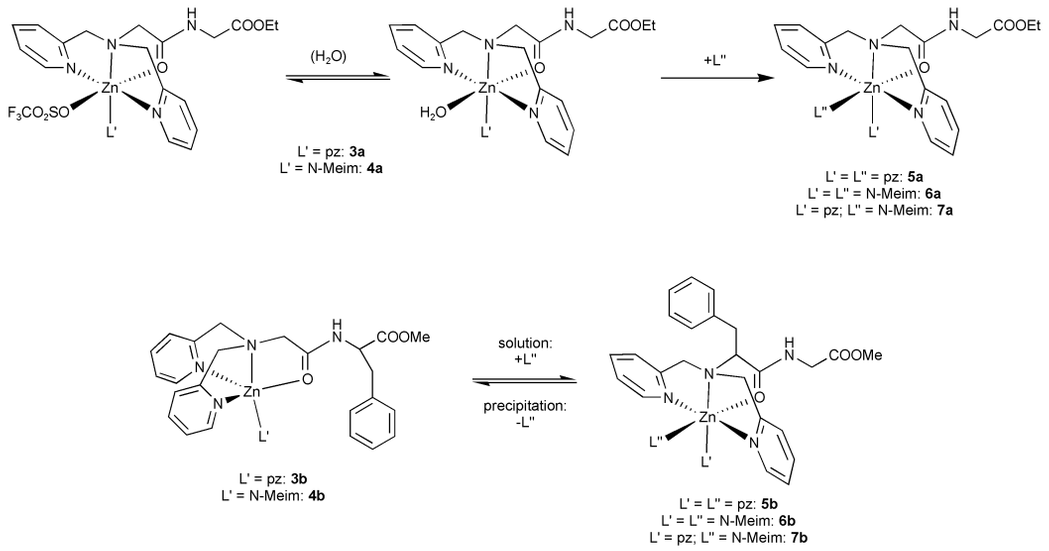

Scheme 2 Synthesis of octahedral zinc complexes with two heterocyclic amine coligands.

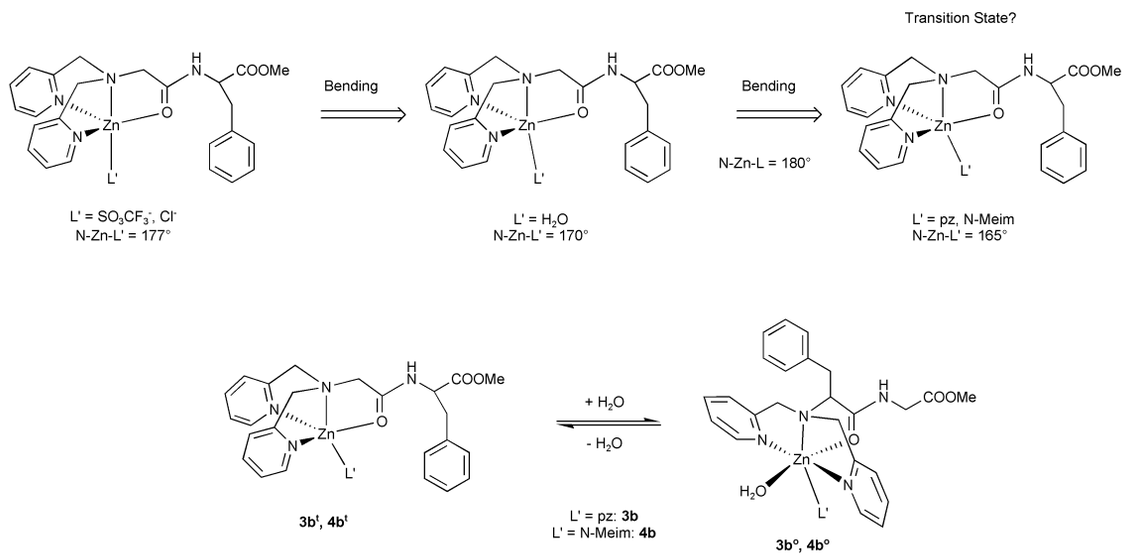

Scheme 3 Complex $\mathbf{3b^t}$ as a transition-state analogue in the conversion of five- to six-coordinate zinc complexes.

Unfortunately, the reactions producing **5a**, **6b**, **7a** and **7b** only resulted in the separation of light yellow oils which did not yield satisfactory elemental analyses data and prevented purification of the products.

Interestingly, repeated re-precipitation of the crude product **5b** resulted in subsequent loss of one equivalent of pyrazole and finally yielded the complexes $\mathbf{3b^t}$. This is a clear indication for the stabilization of five-coordinate structures by aromatic interactions involving the phenylalanine ligand. Isolation of the six-coordinate species is not possible for the phenylalanine derivatives. However, the stabilizing effects are rather weak. In solution, pure $\mathbf{3b^t}$ is readily converted to octahedral species $\mathbf{3b^o}$ (water and/or triflato complexes). This is shown in Scheme 3 and will be discussed in the following NMR section. Even in the absence of an additional heterocyclic amine ligand trace amounts of water bind to the complex. This supports our interpretation of $\mathbf{3b^t}$ as a transition state analogue in the conversion of trigonal-bipyramidal to octahedral zinc complexes in our series. Although $\mathbf{4b^t}$ has not been characterized by X-ray crystallography, it has similar spectroscopic (IR) and analytical properties and is therefore assumed to have a similar structure.

One of our goals was to identify NMR spectroscopic patterns which allow an unequivocal assignment to either five- or six-coordinate structures. Since in our series of bpaAc–Phe–OMe complexes **1b**/**2b** was the only example for a structurally characterized complex which stays trigonal-bipyramidal in solution, we had to include another example to ascertain our interpretations. This was provided by a chloro complex which we knew should be trigonal-bipyramidal. We have synthesized the chloro complex **8a** earlier by reaction of bpaAc–Gly–OEt with zinc(II) chloride.[15] The analogous phenylalanine derivative is also accessible. However, we have observed that the tetrachlorozincate(II) ions obtained by this procedure cause severe problems in spectroscopic investigations. This may be due to the well known formation of a wide array of different structures in solution.[16] In order to study the cation $[(\text{bpaAc–Phe–OMe})\text{Zn(Cl)}]^+$ by NMR spectroscopy we have developed a new route to synthesize the complex **8b** by ligand exchange from **2b** and sodium chloride. This is shown in Scheme 4.

^{1}H NMR spectra

Temperature-dependent ^{1}H NMR experiments in $CDCl_3$ covering the range from −60 to +55 °C have been performed on all complexes described above. COSY spectra were used for the unambiguous assignment of resonance signals. In this section we briefly describe those features which are most relevant for the evaluation of solution structures. The characteristics of the different ligands and structure types are summarized in Table 1 which serves as a guide through the following discussion. According to the NMR spectra of the bpaAc–Phe–OMe complexes at room temperature the compounds can be divided

Table 1 Characteristic ^{1}H NMR properties of the investigated complexes

	bpaAc–Phe–OMe Complexes		bpaAc–Gly–OEt Complexes
Functional group	Trigonal-bipyramidal [(bpaAc–Phe–OMe)ZnL]$^{n+}$ L = OTf^- (**1b**), H_2O (**2b**), Cl^- (**8b**)	Octahedral [(bpaAc–Phe–OMe)ZnL$_2$]$^{n+}$ L = pz, *N*-MeIm (**3b**, **4b**, **5b**, **6b**, **7b**)	[(bpaAc–Phe–OMe)ZnL]$^{n+}$ and [(bpaAc–Phe–OMe)ZnL$_2$]$^{n+}$; L = OTf^- (**1a**), H_2O (**2a**), Cl^- (**8a**), pz, *N*-Meim (**3a**, **4a**, **5a**, **6a**, **7a**)
Phenyl	Ph^4, $Ph^{3,5}$, $Ph^{2,6}$ well resolved; high field shift of Ph^4 to *ca.* 6.6 ppm	Ph^4, $Ph^{3,5}$, $Ph^{2,6}$ not resolved; *ca.* 7.0 ppm	
β-CH_2	$^2J_{HH}$ (1) = *ca.* 11 Hz (*ca.* 2.9 ppm) $^2J_{HH}$ (2) = *ca.* 4.5 Hz (*ca.* 3.3 ppm)	$^2J_{HH}$ (1) = *ca.* 9 Hz (*ca.* 2.9 ppm) $^2J_{HH}$ (2) = *ca.* 6 Hz (*ca.* 3.1 ppm)	
Methylene	4 d for 2 × py–CH_2 and 2 d for C(O)CH_2	1 m for 2 × py–CH_2 and 2 d for C(O)CH_2	generally: 2 d for py–CH_2 and 1 s for C(O)CH_2 **3a**, **7a**: 1 broad signal for py–CH_2, 1 s for C(O)CH_2
Pyridine	2 Sets well resolved; py^6 at *ca.* 9.0 ppm	1 Set; py^6 at *ca.* 7.8 ppm	L = OTf^-, H_2O, Cl^-; py^6 at *ca.* 9.0 ppm L = pz, *N*-Meim: py^6 at *ca.* 7.8 ppm
α-CH	*ca.* 5.1 ppm	*ca.* 4.4 ppm	*ca.* 4.3 ppm
Water (temp. dependent)	Zn-bound (**2b**): 4.0 (30 °C) to 6.5 ppm (−50 °C) free (**8b**): 2.0 (30 °C) to 3.2 (−50 °C)	Zn-bound (**3b**, **4b**): 2.5 (30 °C) to 4.7 ppm (−50 °C) free: 2.0 (30 °C) to 3.2 (−50 °C)	Zn-bound (**1b**): 2.5 (30 °C) to 4.7 ppm (−50 °C) free: 2.0 (30 °C) to 3.2 (−50 °C)
Temperature dependence	Ligand signals do not change significantly with temperature	Ligand signals almost unaffected; coalescence of aromatic heterocycle resonances at low temperature	Ligand signals almost unaffected; coalescence of aromatic heterocycle resonances at low temperature

into two classes. Fig. S1 containing the most characteristic range of the spectra is available as electronic supplementary information. †

1 Benzyl resonances. In the triflato/aqua (**1b/2b**) and chloro (**8b**) complexes the phenyl protons give rise to three well separated sets of signals which are assignable to the positions Ph^4, $Ph^{3,5}$ and $Ph^{2,6}$. Particularly interesting is the significant high field shift of the Ph^4 resonance. This observation is nicely explained by the X-ray structures of our trigonal-bipyramidal complexes **1b**, **2b** and **3b^t**. The Ph^4 proton in all three complexes resides directly above one of the coordinating pyridine ligands and should therefore experience a shift by the aromatic ring current. Thus, the complexes **1b/2b** and **8b** are trigonal-bipyramidal in solution as well as in the solid state. This is further supported by the vicinal coupling constants of the β-CH_2 groups. A large value of *ca.* 11 Hz is observed for the signal at *ca.* 2.9 ppm, whereas the signal at *ca.* 3.3 ppm shows a splitting of only 4.5 Hz. According to the Karplus relationship[17] which is illustrated in Fig. 3, this is in excellent agreement with a rigid staggered conformation with well defined H–α-C–β-C–H dihedral angles of 180 and 60°, respectively. As expected, the difference between the two values increases with decreasing temperatures reflecting the reduced mobility upon cooling. This is shown in Table 2 which contains the temperature-dependent vicinal coupling constants between −10 and +55 °C. The result is remarkable since the benzyl side chain in our complexes is not locked by steric restrictions. A fixed conformation in solution therefore provides good evidence for the relevance of aromatic interactions.

Fig. 3 The Karplus relationship as relevant in complexes of bpaAc–Phe–OMe.

In contrast, all of the complexes with pyrazole or *N*-methylimidazole coligands (**3b^o**, **4b^o**, **5b**, **6b**, **7b**) show only one poorly resolved multiplet assignable to their five phenyl protons. The signal is observed at a typical value of *ca.* 7 ppm. Concomitantly we observe that the vicinal coupling constants of the β-CH_2 groups are closer to the values expected for a statistical angular distribution. These findings are consistent with octahedral structures of the complexes in solution. X-Ray crystallographic data of related copper(II) complexes clearly show that the phenylalanine side chain is free to rotate in square-pyramidal or octahedral complexes.[18] Our NMR results therefore prove that **3b** does not retain its five-coordinate solid state structure but binds an additional sixth ligand. This structural change is presumably driven by solvation effects. To our surprise there is no evidence for an equilibrium between five- and six-coordinate species. Apparently, the distorted octahedral complex **3b^o** is significantly more stable in solution than **3b^t**. This may be explained by a reduction of charge and/or hydrophilic patches on the complex which is certainly favorable in a non-polar solvent such as chloroform. We conclude that the aromatic interactions in our complexes are not strong enough to preserve the tense geometry of **3b^t** if solvation energy effects provide an additional stabilization of a six-coordinate complex **3b^o**.

2 Methylene, pyridine and α-CH-resonances. The signals of the four py–CH_2 and the two C(O)CH_2 protons support the

Table 2 400 MHz ^{1}H NMR chemical shifts (δ, ppm) observed for H_2O in $CDCl_3$ solutions of the complexes

	T/°C	**1a/2a**	**1a/2b**	**3a**	**3b**	**4a**	**4b**	**5a**	**5b**	**6a**	**6b**	**7a**	**7b**	**8b**
	+20	2.6	4.2	2.1	–	2.1	2.5	–	–	2.0	2.0	2.0	–	2.0
	−20	3.9	5.8	3.2	–	3.0	–	–	–	2.6	2.6	2.7	3.3	2.6
	−60	5.9	6.7	4.8	4.9	*ca.* 4.5	4.9	–	–	–	–	–	–	–

Table 3 Vicinal ($^3J_{HH}$/Hz (δ/ppm)) coupling constants for the β-CH_2 groups (ABX spin–system) in the (bpaAc–Phe–OMe) complexes **1b**–**8b** (400 MHz)

		1b/2b		**3b**		**4b**		**5b**		**6b**		**7b**		**8b**	
T/°C	δ	2.83	3.26	2.83	3.04	2.82	3.01	2.82	3.01	2.78	2.94	2.79	2.96	2.94	3.32
55	$^3J_{HH}$	10.3	5.0	8.9	6.0	8.9	6.0	8.8	6.0	8.5	6.1	8.6	6.1	10.6	4.8
20	$^3J_{HH}$	10.9	4.7	9.2	5.8	9.2	5.9	9.1	6.0	8.6	6.2	8.7	6.2	11.1	4.5
−10	$^3J_{HH}$	11.4	4.3	9.5	5.7	9.5	broad	9.0	6.0	8.6	6.3	8.7	6.2	11.6	4.3

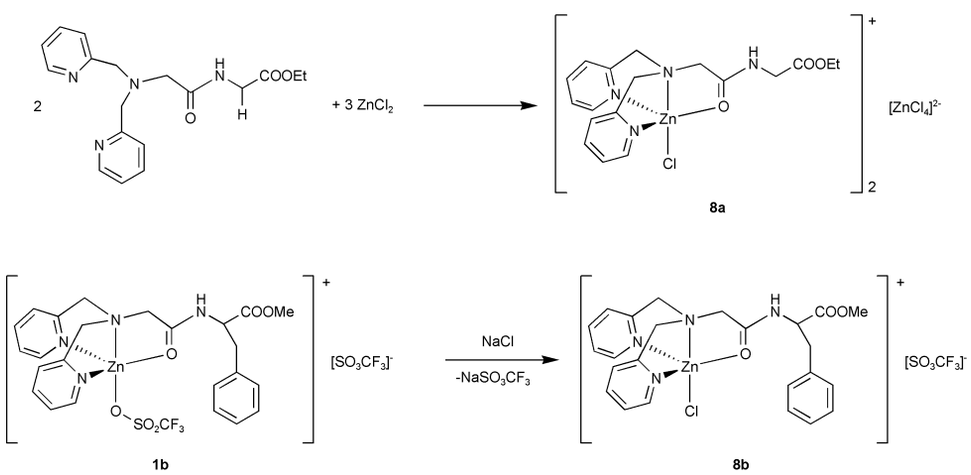

Scheme 4 Synthesis of chloro complexes $[LZnCl]^+$.

structural assignments made above. In the cases of **1b/2b** and **8b** all signals are well resolved. This has been further confirmed by two-dimensional COSY spectra. Thus, the picolyl substituents are inequivalent as is expected for a locked benzyl conformation. The same behavior is seen in the signals of the pyridine protons. Two sets are observed consistent with an asymmetric environment. In contrast, the complexes **3b**^{o}, **4b**^{o}, **5b**, **6b**, **7b** show only one multiplet corresponding to four protons of the py-CH_2 groups. Unfortunately, the signal overlaps with that of the α-CH proton and can therefore not be further resolved. At the same time, only one set of signals is observed for the pyridine proton resonances. This provides additional evidence for octahedral structures with mobile benzyl side chains. Also noteworthy is the large shift difference between the py^6 resonances in the trigonal-bipyramidal (9.0 ppm) and octahedral (7.8 ppm) complexes. Interestingly, the same py^6 shifts are observed in the spectra of the corresponding glycine derivatives. We think that it originates in the ring current of the aromatic heterocyclic coligand which should affect the py^6 proton regardless of the coordination number. Thus, it is not possible to deduce the solution structures of the glycine compounds by a simple analysis of their pyridine resonances. Since the ligand bpaAc–Gly–OEt does not contain a stereogenic center, the pyridine signals always appear as one set of signals.

Another interesting feature is the α-CH resonance. In the trigonal-bipyramidal bpaAc–Phe–OMe complexes it is observed at *ca.* 5.1 ppm, whereas it appears at *ca.* 4.4 ppm in the octahedral complexes. However, the bpaAc–Gly–OEt complexes show their α-CH signal always at 4.3 ppm. Thus, the low field shift in the spectra of **1b/2b** and **8b**, respectively, is most probably a consequence of the benzyl side chain in a trigonal-bipyramidal complex—although we do not have an obvious explanation for this observation. In any case, the α-CH resonance is also not reliable as a criterion for five- or six-coordination in complexes of bpaAc–Gly–OEt.

3 Water resonances. Most of our samples contained at least trace amounts of water giving rise to a relatively broad resonance signal with strongly temperature-dependent chemical shift values. Table 3 contains a summary of these data for all complexes. In some cases we were not able to identify the exact position of the chemical shift due to severe overlap with other signals. These data were left blank. Interestingly, the dipyrazole complexes **5a** and **5b** are the only ones which did not show any sign of water. It should be noted that none of the compounds contained more than 1 equivalent of water and that repeated measurements using samples with different water contents always gave reproducable results. This is important for the validity of the following discussion.

Three distinctly different general cases (A, B, C) can be distinguished. They are exemplified in Fig. 4(a)–(c). A: Free water in samples of the complexes $[(bpaAc–AA–OR)Zn(L')(L'')]^{2+}$ (L = pz, *N*-Meim) gives a signal at *ca.* 2.0 ppm (30 °C) which is shifted to *ca.* 3.2 ppm at low temperature (−50 °C). This is seen in Fig. 4(a) which shows the temperature-dependent spectra of complex **6b**. B: Bound water in octahedral complexes of the type $[(bpaAc–AA–OR)Zn(L')(H_2O)]^{2+}$ has a resonance signal at *ca.* 2.5 ppm (30 °C) which shifts to *ca.* 4.7 ppm at low temperature (−50 °C). An example is provided by complex **4b**, the spectra of which are shown in Fig. 4(b). C: A large shift to lower field strengths is observed for the trigonal-bipyramidal triflato/aqua complex **1b/2b** (Fig. 4(c)). Its water resonance appears at 4.0 ppm (30 °C) and shifts to 6.5 ppm at −50 °C. This value is characteristic for water bound in an axial trigonal-bipyramidal position. The H_2O resonance should

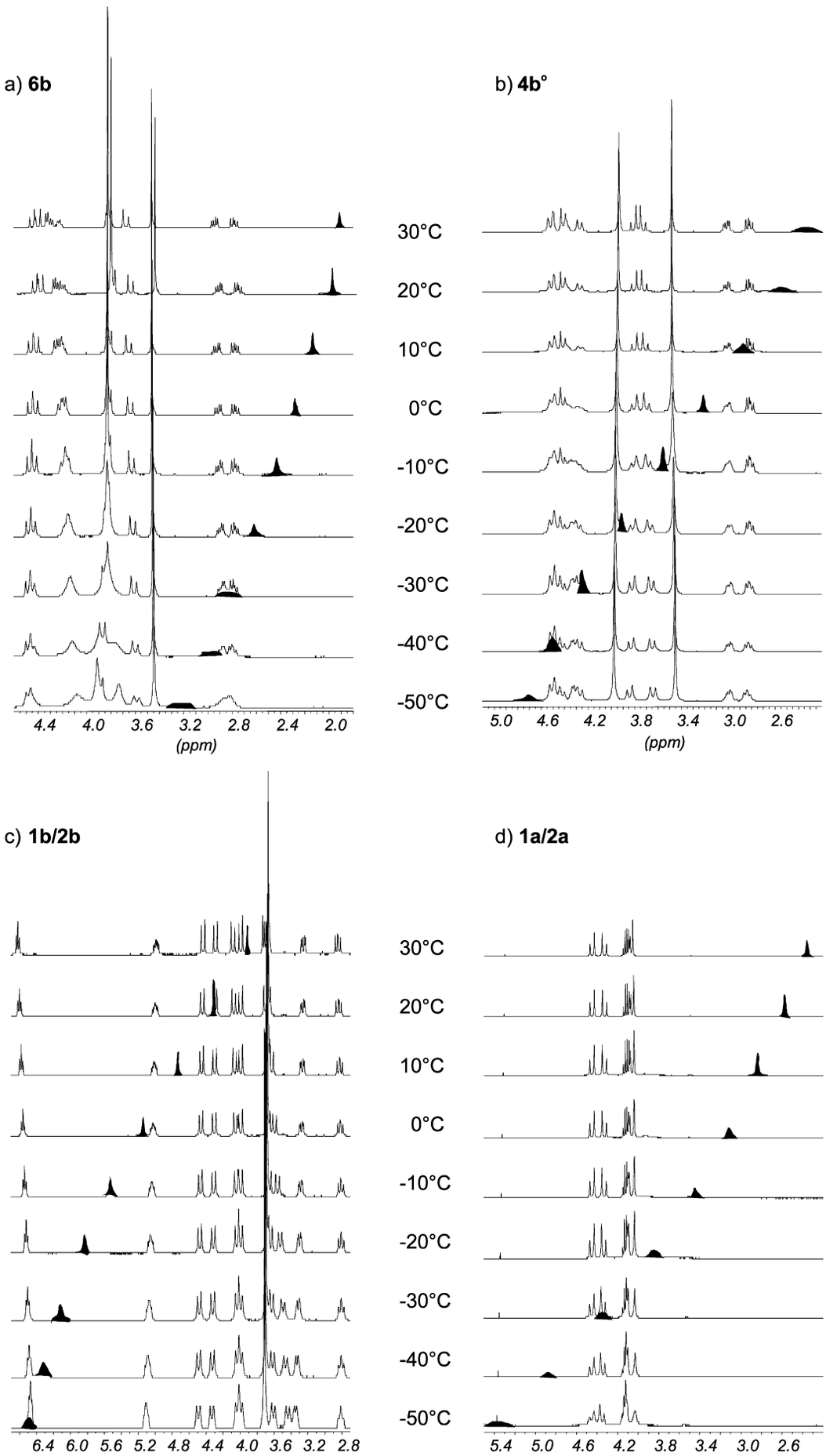

Fig. 4 Proton resonances of water in the temperature-dependent ^{1}H NMR spectra ($CDCl_3$ solutions) of (a) **1a/2a**, (b) **6b**, (c) **4b°** and (d) **1b/2b**; the water signal is marked in black.

therefore be a reliable measure for the structural characterization of aqua complexes in our system.

Fig. 4(d) shows the temperature-dependent spectra of the glycine derivative **1a/1b**. The signal of water appears at 2.5 ppm (30 °C) and shifts to 5.4 ppm (−50 °C). This resembles the behavior of the octahedral complex **4b**[o] more closely than that of the trigonal-bipyramidal complexes **1b/2b**. We therefore propose that the complex is octahedral in solution. This interpretation is indirectly support by the general observation that mononuclear complexes [LZn–OH_2] with L being a tetradentate tripodal N_2O ligand require a special stabilization of their inner coordination sphere by substituents in the ligand periphery.[19] The reported formation of an octahedral diaqua complex with the N_2O ligand dipicolylglycine provides crystallographic evidence for this statement.[20] This is different for symmetric N_3 ligands which readily form trigonal-bipyramidal complexes of the type [LZn–OH_2] without substition at the tripod.[21]

4 Temperature-dependent dynamic effects. The resonance signals of the tripodal ligand bpaAc–Gly–OEt do not change much with temperature. Noteworthy is an asymmetric broadening of the py–CH_2 resonance pattern below 0 °C. This feature is most prominent in the complexes **5a**, **6a** and **7a** which contain two aromatic amine ligands. Thus, only two of the four protons are affected by the corresponding dynamic process. One set of signals is observed for either pyrazole or imidazole in all spectra at room temperature. These resonances become very broad at low temperatures but coalescence is not reached within the range of our measurements. The pyrazole NH signals of **3a**, **5a** and **7a** at *ca.* 13 ppm are only observed at temperatures ≤ −20 °C. The temperature-dependent spectra of the phenylalanine derivatives also show only minor changes of the ligand resonance patterns. Most of the general features are analogous to those observed for the glycine derivatives. The pyrazole and *N*-methylimidazole complexes show the same dynamic behavior as described above.

The temperature-dependent measurements clearly indicate rapid equilibration of (1) the two pyrazole nitrogen atoms and (2) the positions occupied by the two monodentate ligands in **5a**, **5b**, **6a**, **6b**, **7a** and **7b**. Unfortunately, we were not able to access temperatures were these processes are completely frozen. However, one conclusion can be drawn. We have not observed any evidence for a decomplexation of one or more of the tripodal ligand arms. This is different from observations made by Stanbury, Wilson and their coworkers on five-coordinate copper(I) and zinc(II) with pentadentate polyimine ligands.[22] The asymmetric broadening of only one of the two py–CH_2 AB dublets in our complexes clearly shows that only two of the four protons are affected by dynamic processes. We assign the effect to the protons pointing towards the metal ion. They are expected to sense ligand exchange processes at the two active coordination sites of our octahedral complexes.

Conclusions

With its benzyl side chain, the ligand bpaAc–Phe–OMe provides a sensitive ^{1}H NMR spectroscopic probe for structural studies on its zinc complexes in solution. Using it, we were able to confirm that aromatic interactions are relevant in trigonal-bipyramidal complexes. This geometry is characterized by a locked conformation of the benzyl side chain which cannot be explained by steric restrictions. Furthermore, the unusual chemical shift values of the phenyl proton resonances are indicative for a close association between the phenylalanine side chain and one of the pyridine rings in the complexes **1b/2b** and **8b**.

We were also able to provide evidence for the tense character of **3b**[t]. According to the structure correlation concept[23] the distorted trigonal-bipyramidal solid state structure represents a minimum on the hyperpotential surface. However, solvation effects are sufficient to drive the rapid formation of octahedral species **3b**[t] in solution. Thus, the crystalline compound represents a transition state analogue in the conversion of five- to six-coordinate zinc complexes. This interpretation is also supported by the fact that the dipyrazole complex **5b** exists only in solution. One pyrazole ligand is lost upon precipitation.

In summary, much can be learned from our complexes about the stereodynamics of coordination compounds, as well as about effects of weak aromatic interactions which are ubiquitous in biological systems.[3] We will continue our work with a particular focus on a more quantitative description of the fascinating interactions between metal centers and non-coordinating amino acid side chains.

Experimental

General methods

Spectra were recorded with the following instruments: IR: Mattson Polaris FT IR. ^{1}H and ^{13}C NMR: Bruker Avance DPX 300; data reported in the experimental section have been obtained on this instrument. The assignment of ^{1}H NMR signals was assisted by ^{1}H–^{1}H and ^{1}H–^{13}C HMQC spectra. Temperature-dependent ^{1}H NMR measurements: Bruker Avance DRX 400WB. Chemical shifts are referenced to TMS as internal standard, with high frequency shifts recorded as positive. All reactions were carried out under an atmosphere of dry nitrogen. The following workup was performed under ambient laboratory conditions unless stated otherwise. The ligands bpaAc–Gly–OEt and bpaAc–Phe–OMe, as well as the complex salts [(bpaAc–Gly–OEt)Zn(OTf)](OTf) (**1a**) (OTf= SO_3CF_3), [(bpaAc–Gly–OEt)Zn(H_2O)](OTf) (**2a**), [(bpaAc–Phe–OMe)Zn(OTf)](OTf) (**1b**), [(bpaAc–Phe–OMe)Zn(H_2O)](OTf)$_2$ (**2b**),[13] and [(bpaAc–Gly–OEt)Zn(Cl)]$_2$($ZnCl_4$) (**8a**)[14] were prepared as described elsewhere. Details of the preparation of [(bpaAc–Gly–OEt)Zn(pz)(OTf)](OTf) (**3a**), [(bpaAc–Phe–OMe)Zn(pz)](OTf)$_2$ (**3b**), [(bpaAc–Gly–OEt)Zn(*N*-Meim)(H_2O)](OTf)$_2$ (**4a**) and [(bpaAc–Phe–OMe)Zn(*N*-Meim)](OTf)$_2$ (**4b**) have been reported recently.[14] Absolute solvents (CH_2Cl_2, Et_2O, CH_3CN) were purchased from Fluka and stored under nitrogen. Ethylacetate was reagent grade (Roth). All solvents were used without further purification. All other chemicals and deuterated solvents were obtained from Aldrich.

[(bpaAc–Gly–OEt)Zn(*N*-Meim)$_2$](OTf)$_2$ (6a)

The complex **6a** was synthesized by two different methods. The first one started from a reaction of [(bpaAc–Gly–OEt)Zn(H_2O)](OTf)$_2$ (**2a**) with two equivalents of *N*-methylimidazole in acetonitrile. In the second [(bpaAc–Gly–OEt)Zn(*N*-Meim)(H_2O)](OTf)$_2$ (**4a**) was used as the starting material. The latter method afforded higher yields and is therefore described below.

[(bpaAc–Gly–OEt)Zn(*N*-Meim)(H_2O)](OTf)$_2$ (114 mg, 0.14 mmol) was dissolved in 10 ml of acetonitrile. *N*-Methylimidazole (11.1 µl, 0.14 mmol) was added and the solution stirred at room temperature overnight. After removal of all solvent in a vacuum the solid residue was redissolved in a minimum of hot ethylacetate in an ultrasound bath. Slow evaporation of the solvent at room temperature afforded the product as a white precipitate which was collected on a sintered glass filter and dried in a vacuum (106 mg, 0.12 mmol, 86%).

$C_{28}H_{34}F_6N_8O_9S_2Zn$ (870.1 g mol^{-1}): calc.: C 38.65, H 3.94, N 12.88; found: C 38.74, H 4.02, N 12.72%. FAB-MS (nitrobenzylacohol): *m*/*z* = 555 ([(bpaAc–Gly–OEt)Zn(OTf)]$^+$); 405 ([(bpaAc–Gly–OEt)Zn]$^+$). ^{1}H NMR (300 MHz, $CDCl_3$), δ 1.14 (t, 3H, $^3J_{HH}$ = 7.1 Hz, OCH_2CH_3); 1.9 (s, br, H_2O); 3.66 (d, $^3J_{HH}$ = 5.3 Hz, 2H, α-CH_2); 3.78 (s, 2H, C(O)CH_2); 3.83 (s, 6H, 2 × NCH_3); 4.02 (q, 2H, $^3J_{HH}$ = 7.1 Hz, OCH_2CH_3); 4.31, 4.50 (2 × d, 4H, $^2J_{HH}$ = 15.4 Hz, 2 × py–CH_2); 6.95 (s, br, 2H,

2 × H4-im); 7.06 (s, br, 2H, 2 × H5-im); 7.46 (m, 2H, 2 × H5-py); 7.56 (d, 2H, $^3J_{HH}$ = 7.9 Hz, 2 × H3-py); 7.73(s, br, 2H, H2-im); 7.98 (m, 2H, 2 × H4-py); 8.04 (d, 2H, $^3J_{HH}$ = 4.9 Hz, 2 × H6-py); 8.49 (t, $^3J_{HH}$ = 5.3 Hz, 1H, NH). IR (KBr): $\tilde{\nu}$/cm^{-1} = 1744 (COOEt); 1653 (amide I); 1270 (CF_3SO_3).

[(bpaAc–Phe–OMe)ZnCl](OTf) (8b)

[(bpaAc–Phe–OMe)ZnCl](OTf) was obtained through a ligand exchange reaction from [(bpaAc–Phe–OMe)Zn(H_2O)](OTf)$_2$ (**2b**) with NaCl.

[(bpaAc–Phe–OMe)(H_2O)Zn](OTf)$_2$ (320 mg, 0.40 mmol) was dissolved in 5 ml of water. To this solution 5 ml aqueous NaCl (28 mg, 0.48 mmol) was added and the mixture stirred overnight at RT. The resulting clear solution was washed three times with 10 ml CH_2Cl_2. Since the product is very hygroscopic the following workup was carried out under an atmosphere of dry nitrogen. The combined organic layers were dried over $MgSO_4$, filtered, and dried in a vacuum to yield the product as a colorless foam (203 mg, 0.30 mmol, 75%).

$C_{25}ClH_{26}F_3N_4O_6SZn$ (668.4 g mol^{-1}): calc.: C 44.92, H 3.92, N 8.38, S 4.80; found: C 45.09, H 4.00, N 8.28, S 4.49%. FAB-MS (nitrobenzylacohol): *m*/*z* = 518 ([(bpaAc–Phe–OMe)-ZnCl]$^+$). ^{1}H NMR (300 MHz, $CDCl_3$), δ 1.9 (s, br, 1H, H_2O); 2.94 (ABX, $^2J_{HH}$ = 14.0 Hz, $^3J_{HH}$ = 11.1 Hz, 1H, β-CH_2); 3.32 (ABX, $^2J_{HH}$ = 14.0 Hz, $^3J_{HH}$ = 4.4 Hz, 1H, β-CH_2); 3.59 (m, 2H, py–CH(A′)*H*(B′) + C(O)CH(C)*H*(D)); 3.71 (s, 3H, OCH_3); 3.93 (d, $^2J_{HH}$ = 16.4 Hz, 1H, C(O)C*H*(C)H(D)); 3.99 (d, $^2J_{HH}$ = 16.4, 1H, py–CH(A)*H*(B)); 4.13 (d, $^2J_{HH}$ = 16.8, 1H, py–C*H*(A′)-H(B)); 4.28 (d, $^2J_{HH}$ = 16.4, 1H, py–C*H*(A)H(B)); 5.08 (m, 1H, α-CH); 6.72 (m, 1H, H4-Ph); 7.02 (m, 2H, H3,5-Ph); 7.25 (m, 2H, H2,6-Ph); 7,51 (m, 2H, 2 × H3-py); 7.59 (m, 2H, 2 × H5-py); 8.02 (m, 2H, 2 × H4-py); 9.06 (m, 3H, 2 × H6-py + NH). IR (KBr): $\tilde{\nu}$/cm^{-1} = 1747 (COOMe); 1632 (amide I); 1278, 1263 (CF_3SO_3).

General procedure for the syntheses of [(bpaAc–Gly–OEt)Zn-(pz)$_2$](OTf)$_2$ (5a), [(bpaAc–Phe–OMe)Zn(pz)$_2$](OTf)$_2$ (5b) and [(bpaAc–Phe–OMe)Zn(*N*-Meim)$_2$](OTf)$_2$ (6b)

Both methods described for **6a** were used and worked equally well for the synthesis of **5a**, **5b** and **6b**. The reaction mixtures were stirred overnight and dried in a vacuum. It was not possible to purify the crude products since they did not precipitate but rather separated as oils. These solidified as light yellow foams in a vacuum but the solids gave incorrect C,H,N elemental analysis. On that account only the crude products were investigated.

[(bpaAc–Gly–OEt)Zn(pz)$_2$](OTf)$_2$ (5a)

FAB-MS (nitrobenzyl alcohol): *m*/*z* = 555 ([(bpaAc–Gly–OEt)Zn(OTf)]$^+$), 405 ([(bpaAc–Gly–OEt)Zn]$^+$). ^{1}H NMR (300 MHz, $CDCl_3$), δ 1.14 (t, $^3J_{HH}$ = 7.2 Hz, 3H, OCH_2CH_3); 3.79 (d, $^3J_{HH}$ = 5.6 Hz, 2H, α-CH_2); 3.88 (s, 2H, C(O)CH_2); 4.06 (q, $^3J_{HH}$ = 7.2 Hz, 3H, OCH_2CH_3); 4.49, 4.55 (2 × d, $^2J_{HH}$ = 15.8 Hz, 4H, 2 × py–CH_2); 6.55 (s, br, 2H, 2 × H4-pz); 7.40 (m, 2H, 2 × H5-py); 7.53 (d, $^3J_{HH}$ = 7.5 Hz, 2H, 2 × H3-py); 7.83 (m, 6H, 2 × H6-py + 2 × H3-pz + 2 × H5-pz); 7.96 (m, 2H, 2 × H4-py); 8.93 (m, 1H, NH); 12.66 (−60 °C, 1H, NH-pz). IR (KBr): $\tilde{\nu}$/cm^{-1} = 1746 (COOEt); 1638 (amide I); 1279, 1263 (CF_3SO_3).

[(bpaAc–Phe–OMe)Zn(pz)$_2$](OTf)$_2$ (5b)

FAB-MS (nitrobenzyl acohol): *m*/*z* = 632 ([(bpaAc–Phe–OMe)Zn(OTf)]$^+$); 481 ([(bpaAc–Phe–OMe)Zn]$^+$). ^{1}H NMR (300 MHz, $CDCl_3$), δ 2.84 (ABX, $^2J_{HH}$ = 13.9 Hz, $^3J_{HH}$ = 9.0 Hz, 1H, β-CH_2); 3.02 (ABX, $^2J_{HH}$ = 13.9 Hz, $^3J_{HH}$ = 5.9 Hz, 1H, β-CH_2); 3.50 (s, 3H, OCH_3); 3.79, 3.91 (2 × d, $^2J_{HH}$ = 17.6 Hz, 2H, 2 × C(O)CH_2); 4.44 (m, 5H, α-CH + 2 × py–CH_2); 6.61 (m, 2H, H4-pz); 7.03 (m, 5H, Ph); 7.38 (m, 2H, 2 × H5-py); 7.49 (m, 2H, 2 × H3-py); 7.76 (m, 2H, 2 × H6-py); 7.81 (m, 2H, H3-pz + H5-pz); 7.94 (m, 2H, 2 × H4-py); 9.06 (d, $^3J_{HH}$ = 7.1 Hz, 1H, NH); 12.66 (−60 °C, 1H, NH-pz). IR (KBr): nu(tilde) = 1746 (COOMe); 1644 (amide I); 1282, 1257 (CF_3SO_3).

[(bpaAc–Phe–OMe)Zn(*N*-Meim)$_2$](OTf)$_2$ (6b)

FAB-MS (nitrobenzyl alcohol): *m*/*z* = 631 ([(bpaAc–Phe–OMe)Zn(OTf)]$^+$; 481 ([(bpaAc–Phe–OMe)Zn]$^+$). ^{1}H NMR (300 MHz, $CDCl_3$), δ 2.0 (s, br, H_2O); 2.77 (ABX, $^2J_{HH}$ = 13.9 Hz, $^3J_{HH}$ = 8.6 Hz, 1H, β-CH_2); 2.93 (ABX, $^2J_{HH}$ = 13.9 Hz, $^3J_{HH}$ = 6.2 Hz, 1H, β-CH_2); 3.47 (s, 3H, OCH_3); 3.73 (m, 5H, C(O)CH_2 + NCH_3); 4.36 (m, 5H, α-CH + 2 × py–CH_2); 6.89 (s, br, 1H, H4-im); 7.06 (m, 5H, H–Ph + H5-im); 7.48 (m, 4H, 2 × H3-py + 2 × H5-py); 7.72 (s, br, 1H, H2-im); 7.95 (m, 4H, 2 × H4-py + 2 × H6-py); 8.51 (d, $^3J_{HH}$ = 6.8 Hz, 1H, NH). IR (KBr): $\tilde{\nu}$/cm^{-1} 1747 (COOMe); 1657 (amide I); 1275 (CF_3SO_3).

General procedure for the syntheses of [(bpaAc–Gly–OEt)-Zn(*N*-Meim)(pz)](OTf)$_2$ (7a) and [(bpaAc–Phe–OMe)-Zn(*N*-Meim)(pz)](OTf)$_2$ (7b)

The complexes **7a** and **7b** were obtained starting either from the pyrazole complexes **3a** and **3b**, respectively, or from the respective *N*-methylimidazole complexes **4a** and **4b**. These two methods work similarly well for both amino acid derivatives. One equivalent of the aromatic amine was added to a solution of the zinc complex in acetonitrile. The reaction mixture was stirred overnight and dried in a vacuum. Purification of the crude products was not possible since the compounds did not precipitate but rather separated as oils. These solidified as light yellow foams in a vacuum but the solids gave incorrect C,H,N elemental analysis. On that account only the crude products were investigated.

[(bpaAc–Gly–OEt)Zn (*N*-Meim)(pz)](OTf)$_2$ (7a)

FAB-MS (nitrobenzyl alcohol): *m*/*z* = 555 ([(bpaAc–Gly–OEt)Zn(OTf)]$^+$), 405 ([(bpaAc–Gly–OEt)Zn]$^+$). ^{1}H NMR (300 MHz, $CDCl_3$), δ 1.13 (t, $^3J_{HH}$ = 7.1 Hz, 3H, OCH_2CH_3); 2.0 (s, br, H_2O); 3.72 (d, $^3J_{HH}$ = 5.5 Hz, 2H, α-CH_2); 3.83 (s, 2H, C(O)CH_2); 3.88 (s, 3H, NCH_3); 4.01 (q, $^3J_{HH}$ = 7.1 Hz, 3H, OCH_2CH_3); 4.49 (s, 4H, 2 × py–CH_2); 6.48 (s, br, 1H, H4-pz); 7.14 (s, br, 1H, H4-im); 7.22(s, br, 1H, H5-im); 7.40 (m, 2H, 2 × H5-py); 7.53 (d, $^3J_{HH}$ = 7.7 Hz, 2H, 2 × H3-py); 7.75 (d, $^3J_{HH}$ = 1.8 Hz, 2H, H3-pz + H5-pz); 7.96 (m, 4H, 2 × H4-py + 2 × H6-py); 8.04 (s, br, 1H, H2-im); 8.72 (s, br, 1H, NH); 12.37 (−30 °C, 1H, NH). IR (KBr): $\tilde{\nu}$/cm^{-1} = 1746 (COOEt); 1654 (amide I); 1279, 1262 (CF_3SO_3).

[(bpaAc–Phe–OMe)Zn (*N*-Meim)(pz)](OTf)$_2$ (7b)

FAB-MS (nitrobenzyl alcohol): *m*/*z* = 631 ([(bpaAc–Phe–OMe)Zn(OTf)]$^+$); 481 ([(bpaAc–Phe–OMe)Zn]$^+$). ^{1}H NMR (300 MHz, $CDCl_3$), δ 2.79 (ABX, $^2J_{HH}$ = 13.8 Hz, $^3J_{HH}$ = 8.8 Hz, 1H, β-CH_2); 2.96 (ABX, $^2J_{HH}$ = 13.8 Hz, $^3J_{HH}$ = 6.1 Hz, 1H, β-CH_2); 3.47 (s, 3H, OCH_3); 3.69, 3.81 (2 × d, $^2J_{HH}$ = 17.6 Hz, 2H, C(O)CH_2); 3.84 (s, 3H, NCH_3); 4.37 (m, 5H, α-CH + 2 × py–CH_2); 6.44 (s, br, 1H, H4-pz); 7.06 (m, 7H, H–Ph + H4-im + H5-im); 7.41, 7.50 (2 × m, 4H, 2 × H3-py + 2 × H5-py); 7.68 (s, br, 2H, H3-pz + H5-pz); 7.83 (s, br, 1H, H2-im); 7.93 (m, 4H, 2 × H4-py + 2 × H6-py); 8.74 (d, $^3J_{HH}$ = 6.7 Hz, 1H, NH); 12.15 (−60 °C, 1H, NH). IR (KBr): $\tilde{\nu}$/cm^{-1} = 1745 (COOMe); 1656 (amide I); 1280, 1261 (CF_3SO_3).

Acknowledgements

The authors gratefully acknowledge financial support from the Deutsche Forschungsgemeinschaft. We thank Prof. Rudi van Eldik who generously let us share his equipment, laboratory space, and funding.

References

1 O. Yamauchi, A. Odani and M. Takani, *J. Chem. Soc., Dalton Trans.*, 2002, 3411.

2 (*a*) B. Alberts, D. Bray, J. Lewis, M. Raff, K. Roberts and J. D. Watson, *Molecular Biology of the Cell*, Garland, New York, 3rd edn., 1994; (*b*) K. M. Guckian, B. A. Schweitzer, R. X. F. Ren, C. J. Sheils, P. L. Paris, D. C. Tahmassebi and E. T. Kool, *J. Am. Chem. Soc.*, 1996, **118**, 8182; (*c*) K. M. Guckian, B. A. Schweitzer, R. X.-F. Ren, C. J. Sheils, D. C. Tahmassebi and E. T. Kool, *J. Am. Chem. Soc.*, 2000, **122**, 2213.

3 (*a*) S. K. Burley and G. A. Petsko, *FEBS Lett.*, 1986, **203**, 139; (*b*) S. K. Burley and G. A. Petsko, *Science*, 1985, **229**, 23; (*c*) C. A. Hunter and J. K. M. Sanders, *J. Am. Chem. Soc.*, 1990, **112**, 5525; (*d*) J. C. Ma and D. A. Dougherty, *Chem. Rev.*, 1997, **97**, 1303; (*e*) J. P. Gallivan and D. A. Dougherty, *Proc. Natl. Acad. Sci. USA*, 1999, **96**, 9459.

4 S. D. Zaric, D. M. Popovic and E. W. Knapp, *Chem. Eur. J.*, 2000, **6**, 3935.

5 C. Chipot, R. Jaffe, B. Maigret, D. A. Pearlman and P. A. Kollmann, *J. Am. Chem. Soc.*, 1996, **118**, 11217.

6 (*a*) S. L. De Wall, E. S. Meadows, L. J. Barbour and G. W. Gokel, *Proc. Natl. Acad. Sci. USA*, 2000, **97**, 6271; (*b*) S. Y. Jon, J. Kim, M. Kim, S.-H. Park, W. S. Jeon, J. Heo and K. Kim, *Angew. Chem.*, 2001, **113**, 2174.

7 C. Janiak, *J. Chem. Soc., Dalton Trans.*, 2000, 3385.

8 H. Suezawa, T. Yoshida, Y. Umezawa, S. Tsuboyama and M. Nishio, *Eur. J. Inorg. Chem.*, 2002, 3148.

9 (*a*) T. Kiss and Z. Szucs, *J. Chem. Soc., Dalton Trans.*, 1986, 2443; (*b*) O. Yamauchi, A. Odani and H. Masuda, *Inorg. Chim. Acta*, 1992, **198**, 749; (*c*) T. Sugimori, K. Shibakawa, H. Masuda, A. Odani and O. Yamauchi, *Inorg. Chem.*, 1993, **32**, 4951; (*d*) P. Hu, C. Sorensen and M. L. Gross, *J. Am. Soc. Mass Spectrom.*, 1995, **6**, 1079; (*e*) T. Sugimori, H. Masuda, N. Ohata, K. Koiwai, A. Odani and O. Yamauchi, *Inorg. Chem.*, 1997, **36**, 576; (*f*) Y. Shimazaki, H. Yokoyama and O. Yamauchi, *Angew. Chem.*, 1999, **111**, 2561.

10 (*a*) H. Sigel, *Angew. Chem.*, 1975, **87**, 391; (*b*) J. B. Orenberg, B. E. Fischer and H. Sigel, *J. Inorg. Nucl. Chem.*, 1980, **42**, 785; (*c*) R. Malini-Balakrishnan, K. H. Scheller, U. K. Haering, R. Tribolet and H. Sigel, *Inorg. Chem.*, 1985, **24**, 2067.

11 (*a*) H. Okawa, Y. Numata, A. Mio and S. Kida, *Bull. Chem. Soc. Jpn.*, 1980, **53**, 2248–2251; (*b*) G. Arena, R. P. Bonomo, L. Casella, M. Gullotti, G. Impellizzeri, G. Maccarrone and E. Rizzarelli, *J. Chem. Soc., Dalton Trans.*, 1991, 3203.

12 (*a*) A. J. Amoroso, J. C. Jeffery, P. L. Jones, J. A. McCleverty, P. Thornton and M. D. Ward, *Angew. Chem.*, 1995, **107**, 1577; (*b*) A. J. Costa-Filho, O. R. Nascimento, L. Ghivelder and R. Calvo, *J. Phys. Chem. B*, 2001, **105**, 5039.

13 N. Niklas, O. Walter and R. Alsfasser, *Eur. J. Inorg. Chem.*, 2000, 1723.

14 N. Niklas, O. Walter, F. Hampel and R. Alsfasser, *J. Chem. Soc., Dalton Trans.*, 2002, 3367.

15 N. Niklas, S. Wolf, G. Liehr, C. E. Anson, A. K. Powell and R. Alsfasser, *Inorg. Chim. Acta*, 2001, **314**, 126.

16 (*a*) H. Follner, *Z. Anorg. Allg. Chem.*, 1972, **387**, 43; (*b*) M. C. Kerr, H. S. Preston, H. L. Ammon, J. E. Huheey and J. M. Stewart, *J. Coord. Chem.*, 1981, **11**, 111; (*c*) V. K. Bel'sky, N. R. Streltsova, B. M. Bulychev, P. A. Storozhenko, L. V. Ivankina and A. I. Gorbuno, *Inorg. Chim. Acta*, 1989, **164**, 211; (*d*) M. Graf and H. Stoeckli-Evans, *Acta Crystallogr., Sect. C*, 1994, **50**, 1461.

17 T. D. W. Claridge, *High Resolution NMR Techniques in Organic Chemistry*; Pergamon Press, New York, 1999.

18 N. Niklas, F. Hampel, O. Walter, G. Liehr and R. Alsfasser, *Eur. J. Inorg. Chem.*, 2002, 1839.

19 (*a*) G. Parkin, *Chem. Commun.*, 2000, 1971; (*b*) A. Trösch and H. Vahrenkamp, *Inorg. Chem.*, 2001, **40**, 2305.

20 A. Abufarag and H. Vahrenkamp, *Inorg. Chem.*, 1995, **34**, 2207.

21 (*a*) T. Brandsch, F. A. Schell, K. Weis, M. Ruf, B. Mueller and H. Vahrenkamp, *Chem. Ber.*, 1997, **130**, 283–289; (*b*) M. M. Ibrahim, N. Shimomura, K. Ichikawa and M. Shiro, *Inorg. Chim. Acta*, 2001, **313**, 125.

22 D. K. Coggin, J. A. González, A. M. Kook, D. M. Stanbury and L. J. Wilson, *Inorg. Chem.*, 1991, **30**, 1115.

23 (*a*) E. L. Muetterties and L. J. Guggenberger, *J. Am. Chem. Soc.*, 1974, **96**, 1748; (*b*) H.-B. Bürgi and J. D. Dunitz, Structure Correlation, VCH, Weinheim, 1993; (*c*) T. Auf der Heyde, *Angew. Chem.*, 1994, **106**, 871.